Matlab-Based Virtual Wedge Scattering Tool for the Comparison of High Frequency Asymptotics and FDTD Method

Mehmet Alper Uslu, Levent Sevgi

Department of Electronics and Communication Engineering
Dogus University, Istanbul, Acibadem 34722, Turkey
alpuslu@gmail.com, lsevgi@dogus.edu.tr

Abstract ─ A novel Matlab-based diffraction tool for the investigation of scattered fields around a two-dimensional Perfectly Electric Conductor (PEC) wedge is introduced. Analytical (Exact by Integral, as well as some High Frequency Asymptotic (HFA) techniques) and numerical (Finite-Difference Time-Domain (FDTD)) models are included. The FDTD staircase modeling problems are removed by the application of Dey-Mittra Conformal approach.

Index Terms - conformal FDTD, Dey-Mittra, FDTD, hard boundary condition, high frequency asymptotics, scattering, soft boundary condition, staircase modeling, wedge diffraction.

I. INTRODUCTION

The two-dimensional (2D) wedge diffraction is a canonical problem and plays a fundamental role in the construction of High Frequency Asymptotic (HFA) techniques [1-8]. It has been revisited several times for the last couple of decades. One of these revisits is presented in [9] where several HFA techniques, such as Geometric Optics (GO), Physical optics (PO), Physical Theory of Diffraction (PTD), Uniform Theory of Diffraction (UTD), and Parabolic Equation (PE), are compared with each other and advantages/disadvantages are listed. A Matlab-based HFA numerical tool has also been introduced [10]. Numerical difficulties in and alternative computational approaches for complex diffraction integrals and series summation models are discussed in [11]. Finally, a novel, Finite-Difference Time-Domain (FDTD) - based multi-step numerical diffraction coefficient calculation method based on the has been introduced in [12].

A novel Matlab based WedgeFDTD package is introduced in this study. The package uses the multi-step FDTD approach presented in [12] and results are compared against available exact and HFA models. Deficiencies of staircase discretization are removed by the application of Dey-Mittra Conformal Technique [14].

The 2D wedge scattering scenario is pictured in Fig. 1. The polar coordinates r,φ,z are used throughout the paper. The z-axis is aligned along the edge of the wedge. The angle φ is measured from the top face of the wedge. The exterior angle of the wedge equals α. The wedge is illuminated by a Line Source (LS). Source and observer points are (r_0,φ_0) and (r,φ), respectively.

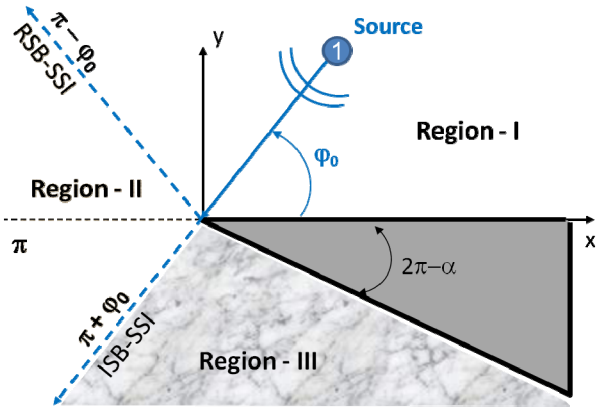

Fig. 1. The 2D PEC wedge problem, line Source (LS) illumination and three characteristic regions separated by RSB and ISB.

Submitted On: Feb. 10, 2012
Accepted On: Aug. 5, 2012

The scenario in Fig. 1 ($0<\varphi_0<\pi$) belongs to the Single Side Illumination (SSI) where *the top face is always illuminated*. The three regions are separated by two critical boundaries; *Incident Shadow Boundary* – ISB ($\varphi=\pi+\varphi_0$), *Reflection Shadow Boundary* – RSB ($\varphi=\pi-\varphi_0$). All field components – incident, reflected and diffracted fields – exist in Region–I. In Region–II, only incident and diffracted fields exist. Only diffracted fields exist in Region–III.

If the source is in ($\alpha-\pi<\varphi_0<\pi$), *both faces are always illuminated* and this is called Double Side Illumination (DSI). In this case, all three field components exist in regions $(0\le\varphi<\pi-\varphi_0)$ and $(2\alpha-\pi-\varphi_0\le\varphi<\alpha)$. There is no reflected field in $(\pi-\varphi_0\le\varphi<2\alpha-\pi-\varphi_0)$.

The field (for $\exp(-i\omega t)$) outside the wedge satisfies

$$\left(\frac{\partial^2}{\partial r^2}+\frac{1}{r}\frac{\partial}{\partial r}+\frac{1}{r^2}\frac{\partial^2}{\partial\varphi^2}+k^2\right)u = \frac{I_0}{r}\delta(r-r_0)\delta(\varphi-\varphi_0). \tag{1}$$

the Boundary Conditions (BC)

$$u_s=0 \text{ or } \partial u_k/\partial n=0 \text{ on } \varphi=0,\alpha. \tag{2-a}$$

and the Sommerfeld's Radiation Condition (SRC) at infinity:

$$\lim_{r\to\infty}\sqrt{kr}\left(\frac{du}{dr}-iku\right)=0. \tag{2-b}$$

Function u_s represents the z-component of electric field intensity E_z (TM), while function u_h is the z-component of magnetic field intensity H_z (TE), which, in acoustics, refer to acoustically soft (SBC) and hard (HBC) wedges, respectively.

II. ANALYTICAL MODELS

The problem has analytical exact as well as HFA solutions. Only analytical exact solution by integral and UTD model are given; the rest can be found in [9-12].

A. Exact solution by integral

The diffracted field solutions with SBC and HBC for both SSI and DSI are presented by Bowman and Senior in handbook [16] as:

$$u_s^{d,BS}=\{V_d(-\pi-\varphi+\varphi_0)-V_d(\pi-\varphi+\varphi_0)\}-\{V_d(-\pi-\varphi-\varphi_0)-V_d(\pi-\varphi-\varphi_0)\}, \tag{3-a}$$

$$u_s^{d,BS}=\{V_d(-\pi-\varphi+\varphi_0)-V_d(\pi-\varphi+\varphi_0)\}+\{V_d(-\pi-\varphi-\varphi_0)-V_d(\pi-\varphi-\varphi_0)\}, \tag{3-b}$$

where

$$V_d(\beta)=\frac{1}{2\pi n}\int_0^\infty H_0^{(1)}[kR(it)]\frac{\sin(\beta/n)}{\cosh(t/n)-\cos(\beta/n)}dt \tag{3-c}$$

$$n=\alpha/\pi,\ R(\eta)=\sqrt{r^2+r_0^2+2rr_0\cos(\eta)}.$$

Total fields $u_{s,h}^{t,BS}$ can be obtained by adding GO fields

$$u_{s,h}^{t,BM}/u_0=\left(u_{s,h}^{d,BM}+u_{s,h}^{GO}\right)/u_0, \tag{4}$$

where GO field that under LS excitation is given as follows:

$$u_{s,h}^{GO}=\begin{cases}H_0^{(1)}(kR_1)\pm H_0^{(1)}(kR_2), & 0\le\varphi<\pi-\varphi_0\\ H_0^{(1)}(kR_1), & \pi-\varphi_0\le\varphi<\pi+\varphi_0.\\ 0, & \pi+\varphi_0\le\varphi\le\alpha\end{cases} \tag{5-a}$$

for SSI and

$$u_{s,h}^{GO}=\begin{cases}H_0^{(1)}(kR_1)\pm H_0^{(1)}(kR_2), & 0\le\varphi<\pi-\varphi_0\\ H_0^{(1)}(kR_1), & \pi-\varphi_0\le\varphi<2\alpha-\pi-\varphi_0.\\ H_0^{(1)}(kR_1)\pm H_0^{(1)}(kR_3), & 2\alpha-\pi-\varphi_0\le\varphi\le\alpha\end{cases} \tag{5-b}$$

for DSI.

B. The UTD Model

The UTD diffracted fields are in the form of

$$u_{s,h}^{d,UTD}=u_0 d_{s,h}^{UTD}\frac{e^{-jkr}}{\sqrt{r}}. \tag{6}$$

where $u_0=H_0^{(2)}(kr_0)$ and the time dependence is $e^{j\omega t}$ [6]. According to the UTD, the diffraction coefficients for SBC and HBCs with line source as follows:

$$d_s^{UTD}(r,\varphi,\varphi_0,k)=$$

$$\frac{-e^{-j\pi/4}}{2n\sqrt{2\pi k}}\left[\begin{array}{l}\cot\left(\frac{\pi-\xi^-}{2n}\right)F\left(kLg^+(\xi^-)\right)\\+\cot\left(\frac{\pi+\xi^-}{2n}\right)F(kLg^-(\xi^-))\\-\cot\left(\frac{\pi-\xi^+}{2n}\right)F\left(kLg^+(\xi^+)\right)\\-\cot\left(\frac{\pi+\xi^+}{2n}\right)F\left(kLg^-(\xi^+)\right)\end{array}\right], \quad (7\text{-a})$$

$$d_h^{UTD}(r,\varphi,\varphi_0,k)=$$

$$\frac{-e^{-j\pi/4}}{2n\sqrt{2\pi k}}\left[\begin{array}{l}\cot\left(\frac{\pi-\xi^-}{2n}\right)F\left(kLg^+(\xi^-)\right)\\+\cot\left(\frac{\pi+\xi^-}{2n}\right)F\left(kLg^-(\xi^-)\right)\\+\cot\left(\frac{\pi-\xi^+}{2n}\right)F\left(kLg^+(\xi^+)\right)\\+c\cot\left(\frac{\pi+\xi^+}{2n}\right)F\left(kLg^-(\xi^+)\right)\end{array}\right], \quad (7\text{-b})$$

where $\xi^+=\varphi+\varphi_0$, $\xi^-=\varphi-\varphi_0$ and the Fresnel function is

$$F(X)=2j\sqrt{X}e^{jX}\int_{\sqrt{X}}^{\infty}e^{-j\tau^2}d\tau. \quad (8)$$

L, $g^{\pm}$ are determined as given in [13] by:

$$L=\frac{rr_0}{(r+r_0)}, g^{\pm}(\xi)=2\cos^2\left(\frac{2n\pi N^{\pm}-\xi}{2}\right). \quad (9)$$

Here, $N^{\pm}=\left(\pm\pi+\xi\right)/\left(2n\pi\right)$ are the integers which most nearly satisfy the last equation given in (9). Note that, the cotangent functions in (7) become singular at ISB/RSB and are replaced with [6]:

$$\cot\left(\frac{\pi\pm\beta}{2n}\right)F\left(kLg^{\pm}(\xi)\right)\simeq$$
$$n\left[\sqrt{2\pi kL}\,\mathrm{sgn}(\varepsilon)-2kL\varepsilon e^{-j\frac{\pi}{4}}\right]e^{-j\frac{\pi}{4}} \quad (10)$$

for small ε. The UTD based total fields are then obtained by adding the GO fields appropriately:

$$u_{s,h}^{t,UTD}/u_0=u_{s,h}^{d,UTD}/u_0+u_{s,h}^{GO}, \quad (11)$$

with the GO solutions given as for SSI ($0<\varphi_0<\alpha-\pi$)

$$u_{s,h}^{GO}=\begin{cases}e^{jkr\cos(\varphi-\varphi_0)}\pm e^{jkr\cos(\varphi+\varphi_0)}, & 0\le\varphi<\pi-\varphi_0\\ e^{jkr\cos(\varphi-\varphi_0)}, & \pi-\varphi_0\le\varphi<\pi+\varphi_0\\ 0, & \pi+\varphi_0\le\varphi\le\alpha\end{cases} \quad (12\text{-a})$$

and for DSI ($\alpha-\pi<\varphi_0<\pi$)

$$u_{s,h}^{GO}=\begin{cases}e^{jkr\cos(\varphi-\varphi_0)}\pm e^{jkr\cos(\varphi+\varphi_0)}, & 0\le\varphi<\pi-\varphi_0\\ e^{-jkr\cos(\varphi-\varphi_0)}, & \pi-\varphi_0\le\varphi<2\alpha-\pi-\varphi_0\\ e^{jkr\cos(\varphi-\varphi_0)}\pm e^{jkr\cos(2\alpha-\varphi-\varphi_0)}, & 2\alpha-\pi-\varphi_0\le\varphi\le\alpha\end{cases} \quad (12\text{-b})$$

Two examples are given in Figs. 2 and 3, where analytical exact solution is compared against the UTD model. Both total and diffracted field variations around the wedge are plotted. Figures 2 and 3 belong to DSI/HBC and SSI/SBC, respectively. Angles of incidences in these plots are 110º and 90º, respectively. As observed, results agree very well [10].

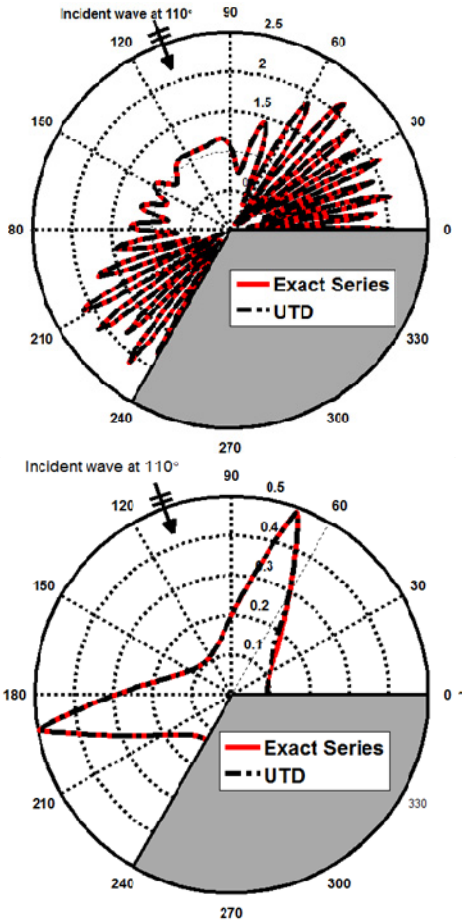

Fig. 2. (Top) Total, (Bottom) Diffracted fields around the PEC wedge; Exact by series vs. UTD

solution (HBC, $\alpha = 240^\circ$, f=30MHz, r=50m, kr=31.4).

III. FDTD MODEL

The Finite-Difference Time-Domain (FDTD) method is a pure numerical technique where Maxwell equations are directly discretized in the time-domain. Since its first introduction [13], it has been widely used in variety of EM problems. A general, multi-step FDTD-based diffraction model under the line source illumination is introduced in [12] where diffracted fields under any *source/observer locations* can be extracted. Results are calibrated via comparisons against analytical exact solutions as well as the UTD and PE models.

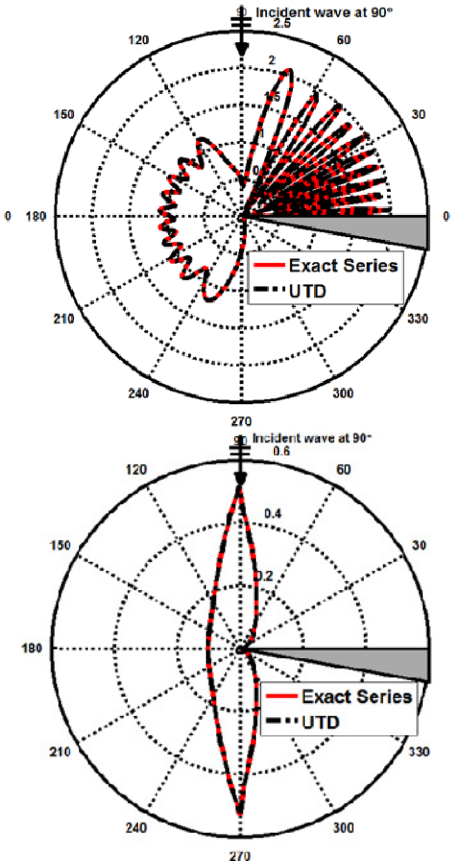

Fig. 3. (Top) Total, (Bottom) Diffracted fields around the PEC wedge; Exact by series vs. UTD solution (SBC, $\alpha = 350^\circ$, f=30MHz, r=50m, kr=31.4).

The FDTD-based wedge scattering model uses one of the two cases presented in Fig. 4. Here, a line source is injected to the E_z (H_z) component in the TM_z (TE_z) model.

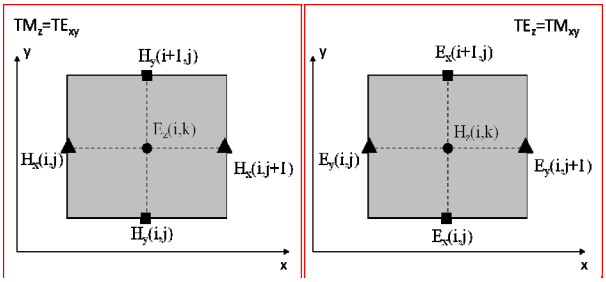

Fig. 4. The 2D FDTD cells on the xy-plane and locations of the field components.

The 2D–FDTD (TM_z type, i.e., soft BC) equations (with H_x, H_y, and E_z components) on the discrete xy–domain are:

$$H_x^{\tilde{n}}(i,j) = \frac{2\mu - \sigma_m \Delta t}{2\mu + \sigma_m \Delta t} H_x^{\tilde{n}-1}(i,j) + \frac{1}{2\mu + \sigma_m \Delta t} \frac{2\Delta t}{\Delta y} \left[E_z^n(i,j+1) - E_z^n(i,j) \right]. \quad (13)$$

$$H_y^{\tilde{n}}(i,j) = \frac{2\mu - \sigma_m \Delta t}{2\mu + \sigma_m \Delta t} H_y^{\tilde{n}-1}(i,j) + \frac{1}{2\mu + \sigma_m \Delta t} \frac{2\Delta t}{\Delta x} \left[E_z^n(i+1,j) - E_z^n(i,j) \right]. \quad (14)$$

$$E_z^n(i,j) = \frac{2\varepsilon - \sigma_e \Delta t}{2\varepsilon + \sigma_e \Delta t} E_z^{n-1}(i,j) + \frac{1}{2\varepsilon + \sigma_e \Delta t} \frac{2\Delta t}{\Delta x} \left[H_x^{\tilde{n}}(i,j) - H_x^{\tilde{n}}(i-1,j) \right] + \frac{1}{2\varepsilon + \sigma_e \Delta t} \frac{2\Delta t}{\Delta y} \left[H_y^{\tilde{n}}(i,j) - H_y^{\tilde{n}}(i,j-1) \right]. \quad (15)$$

The 2D–FDTD (TE_z type, i.e., hard BC) equations (with E_x, E_y, and H_z components) on the discrete xy–domain are

$$E_x^n(i,j) = \frac{2\varepsilon - \sigma_e \Delta t}{2\varepsilon + \sigma_e \Delta t} E_x^{n-1}(i,j) + \frac{1}{2\varepsilon + \sigma_e \Delta t} \frac{2\Delta t}{\Delta y} \left[H_z^{\tilde{n}}(i,j+1) - H_z^{\tilde{n}}(i,j) \right]. \quad (16)$$

$$E_y^n(i,j)=\frac{2\varepsilon-\sigma_e\Delta t}{2\varepsilon+\sigma_e\Delta t}E_y^{n-1}(i,j)+\frac{1}{2\varepsilon+\sigma_e\Delta t}\frac{2\Delta t}{\Delta x}\left[H_z^{\tilde{n}}(i+1,j)-H_z^{\tilde{n}}(i,j)\right]. \quad (17)$$

$$H_z^{\tilde{n}}(i,j)=\frac{2\mu-\sigma_m\Delta t}{2\mu+\sigma_m\Delta t}H_z^{\tilde{n}-1}(i,j)+\frac{1}{(2\mu+\sigma_m\Delta t)}\frac{2\Delta t}{\Delta x}\left[E_x^n(i,j)-E_x^n(i-1,j)\right]+\frac{1}{(2\mu+\sigma_m\Delta t)}\frac{2\Delta t}{\Delta y}\left[E_y^n(i,j)-E_y^n(i,j-1)\right]. \quad (18)$$

Here, i and j are labels of the discrete mesh points, Δx and Δy are the mesh sizes along x and y axes, respectively, and Δt is the time step. Medium parameters are permittivity (ε), permeability (μ), and conductivity (σ). Note, $\tilde{n}=n+1/2$ refer to $\Delta t/2$ time delay between electric and magnetic field computation time instants [13].

According to the method presented in [12] the diffracted fields are extracted for SSI as follows:

- First, FDTD is run for the PEC wedge and scattered fields are stored at n-receivers located on a circular path around the tip. This yields total fields; incident, reflected, and diffracted field components in Region II; and only the diffracted fields in Region III.
- Then, the wedge is removed, FDTD is run for free-space and scattered fields are stored with the same receivers. This yields incident fields all around.
- Finally, bottom face of the wedge is removed and top face is stretched to take up the entire transversal section of simulation space. Then, FDTD is run for the third time. The stored fields yield reflected fields on the upper half-plane.

The three pulses - the incident $u_h^{inc,FDTD}$, reflected $u_h^{\mathrm{Re}fl,FDTD}$, and diffracted $u_h^{d,FDTD}$ - are obtained using the three-step stored data. The related diffracted fields in the frequency domain are then extracted by the application of Fast Fourier Transform (FFT) as $u^d(f)=FFT\{u^{d,FDTD}(t)\}$. For DSI, a replica of third step is requires for the bottom face of the wedge. The numerical diffraction coefficient is then obtained via

$$d_h^{FDTD}=\frac{FFT\left\{u_h^{d,FDTD}\right\}}{FFT\left\{u_h^{inc,FDTD}\right\}}\frac{\sqrt{r}}{e^{ikr}} \quad (19)$$

IV. DISCRETIZATION AND DEY-MITTRA APPROCH

The FDTD procedure summarized above is calibrated against analytical exact as well as HFA models. It is shown that the method works very well under arbitrary source/ observer locations with the standard Yee model using the staircase discretization, except for angles near the bottom face of the wedge. In staircase approximation, when the center of cubic cell is embedded inside the PEC object, all surrounding electric fields of this cell are set to zero. The TM mode fits perfectly with the staircase approximation because tangential electric fields coincide with the third dimension. On the other hand, the TE mode is problematic as illustrated in Fig. 5. As observed, the staircase approximation leads to spurious diffracted fields which can erroneously alter results significantly.

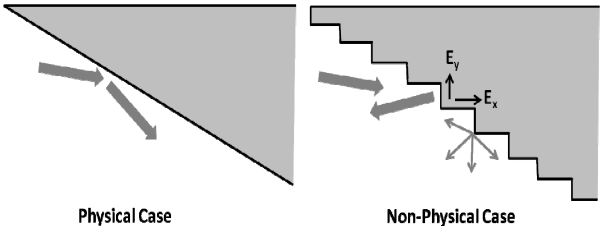

Fig. 5. Physical and non-physical case for the TE_z problem (thick arrows show incident and reflected waves, thin arrows show tip-diffracted waves).

In general, one can neglect staircase approximation error by selecting sampling resolution greater than $\lambda/60$. However, this increases computational burden proportionally and it is not suitable method for dealing with large problems and problems where phase information is crucial (as many as $\lambda/100$ may not be adequate).

Several methods are proposed to overcome staircase problems. Non-uniform gridding based on using smaller cells around the object is one approach, but the pay-off is the increase in total

number of FDTD cells and memory. Another approach is to use conformal FDTD models based on integration contour deformation around curved object being modeled and applying Faraday's law. Then, cell shape is changed to fit boundaries of modeled object. Among existing conformal models, Dey-Mittra technique described in [14] is found to be the most effective one here for the wedge problem. Fundamental steps of the Dey-Mittra technique are summarized below through cases shown in Fig. 6.

In Fig. 6a, slanted object cross slightly into top right cell. If the parameter $s/(\Delta x\Delta y)$ (s is the small area in the figure) is less than R_1 (which is the key parameter specifying numerical stability) one can neglect this penetration and set all four surrounding electric fields to zero for the top right cell. On the other hand, if Faraday's law is applied and integrated along the contour of area A_1 for top left cell one can obtain:

$$H_z^{n+1/2}(-\Delta/2,\Delta y/2)=H_z^{n-1/2}(-\Delta/2,\Delta y/2) + \frac{\Delta t}{\mu_0 A1}\begin{pmatrix} E_y^n(-\Delta x,\Delta y/2)\Delta y + \\ E_x^n(-\Delta x/2,\Delta y)f - E_x^n(-\Delta x/2,0)g \end{pmatrix} \quad (20)$$

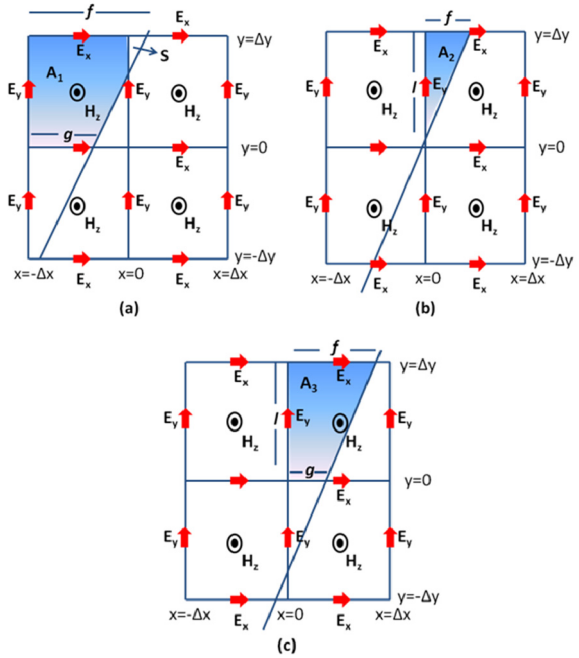

Fig. 6. Dey-Mittra conformal FDTD scenarios.

In Fig. 6b, the ratio of $A_2/(\Delta x\Delta y)$ is larger than R1. In this case, applying Faraday's Law to the top right cell and integrating over the contour of area A_2 gives the update equation for H_z on the top right cell despite the fact that it is in PEC. Noting that two electric field components reside in PEC and set to zero we have:

$$H_z^{n+1/2}(\Delta/2,\Delta y/2)=H_z^{n-1/2}(\Delta/2,\Delta y/2) + \frac{\Delta t}{\mu_0 A2}\left(E_y^n(0,\Delta y/2)l + E_x^n(\Delta x/2,\Delta y)f\right) \quad (21)$$

In Fig. 6c, applying Faraday's law and integrating along over the contour of area A_3 gives:

$$H_z^{n+1/2}(\Delta/2,\Delta y/2)=H_z^{n-1/2}(\Delta/2,\Delta y/2) + \frac{\Delta t}{\mu_0 A3}\begin{pmatrix} E_y^n(0,\Delta y/2)\Delta y \\ +E_x^n(\Delta x/2,\Delta y)f - E_x^n(\Delta x/2,0)g \end{pmatrix} \quad (22)$$

Despite its accuracy of modeling curved or slanted objects, Dey-Mittra conformal technique can cause instabilities. For this reason, time step should be reduced depending on the required accuracy. Stability analyses of several conformal methods are investigated in [15]. Here, selection of the key parameter R_1=0.0025 requires %30 reduction of time step below the normal limit of stability. Another handicap of using Dey-Mittra conformal technique is that it requires complex mesh generation for calculating intersection points of unit cells and boundaries of the object modeled.

Figure 7 compares Dey-Mittra and staircase discretization models. Here, a 60° wedge is illuminated with a line source at 160°. As observed in Fig. 6a, simulation results with Dey-Mittra conformal FDTD model agrees very well with analytical exact solution everywhere. On the other hand, staircase approximation significantly fails to yield correct behavior near the bottom face of the wedge. Things will get worse when both faces of wedge illuminated (DSI). Dey-Mittra conformal FDTD method fits exact results well.

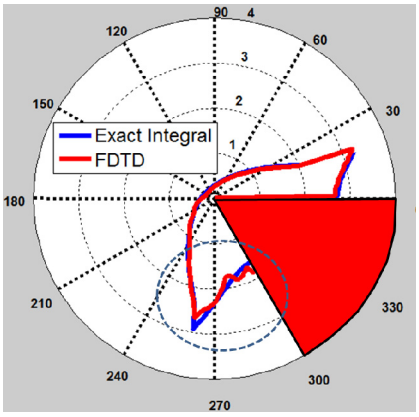

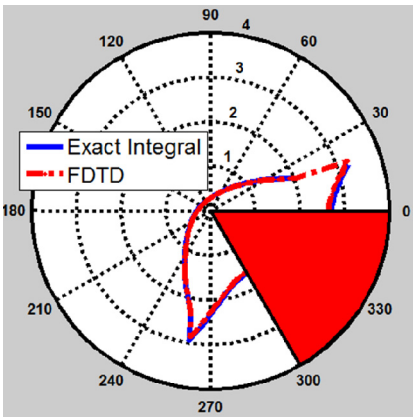

Fig. 7. Exact Solution vs. FDTD for (Top) Staircase approximation (Bottom) Dey-Mittra model.

V. THE WedgeFDTD PACKAGE AND EXAMPLES

A novel Matlab-based WedgeFDTD package with the front panel given in Fig. 8 (showing a time instant just before cylindrical waves emanating from a line source hits the top of the wedge) is developed to simulate scattered fields for a 2D PEC wedge. Results are compared against analytical exact integral method as well as the UTD model. The wedge is discretized with the Dey-Mittra approach. The program is designed with using both Matlab and Java swing library components. The interface of the program is divided into two panels as left and right. The user can enter the FDTD and simulation parameters from the left panel. At the bottom of this panel, user may select simulation results and visualization of different wave pieces. Figure 9 shows a late time instant, showing all – incident, reflected and diffracted – field components. The right panel is reserved for the FDTD visualization and simulation results. Three tabs are placed at top for this purpose.

The tabs are activated after the corresponding simulation type is clicked from the left panel. Also user can select the color map used for FDTD visualization from the popup menu which is placed at top right of this panel. Video recording property is embedded in program via external Mencoder application to reduce video size. For this purpose, one can use the record button which placed at left top of this panel. Bottom panel is dedicated for progress information of the simulation and dynamically appears while the simulation is running. The slider which separates the left and right panel enables enlarging/compressing panel sizes via horizontal scrolling. User can also export simulation results by using the standard MatLab figure toolbar.

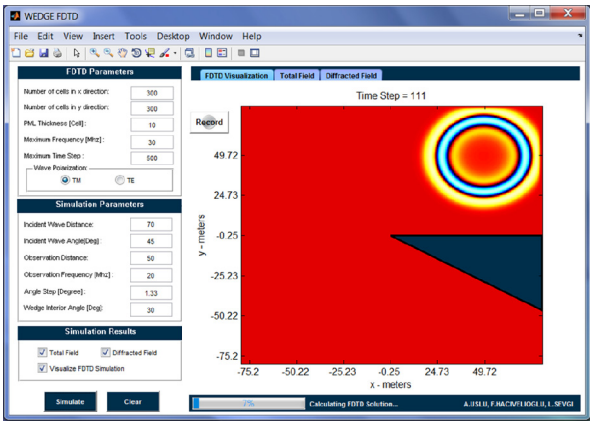

Fig. 8. The front-panel of WedgeFDTD Package.

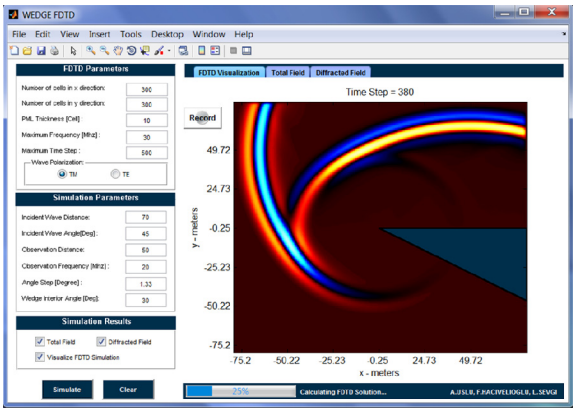

Fig. 9. The front-panel of WedgeFDTD Package showing reflected and tip-diffracted waves.

A few examples are included here. The first example is a TM_z EM or soft BC acoustic problem and belongs to a scenario with a $60°$ wedge apex angle, illuminated by a 20 MHz line source located 70 meters from the tip with the incidence angle $120°$. Total and diffracted fields are shown in Figs. 10 and 11, respectively.

The second example is a TE_z EM or Hard BC acoustic problem which belongs to a wedge with $30°$ interior angle, illuminated with a 30 MHz line source whose distance from the wedge is 80 meters and incidence angle is $45°$ W. The total and diffracted fields are observed at a distance of 50m. Results are given in Figs. 12 and 13, respectively.

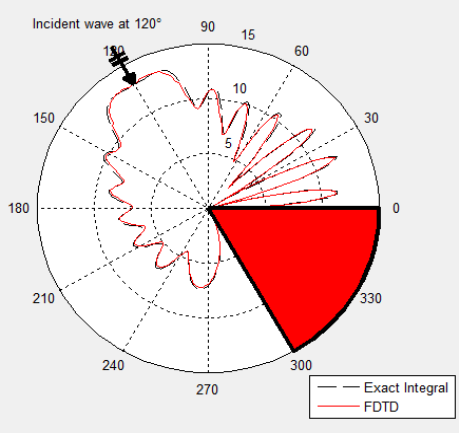

Fig. 10. Total Fields vs. angle computed with both FDTD and exact integral models ($\alpha = 300^{\circ}$, f=20MHz, r=70m, $\varphi_0 = 120^{\circ}$).

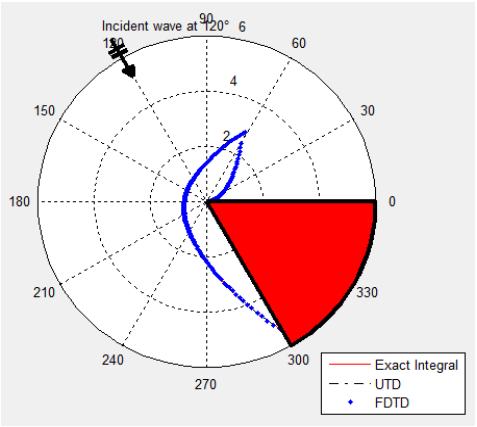

Fig. 11. Diffracted fields vs. angle solution computed with the FDTD, UTD and exact integral models ($\alpha = 300^{\circ}$, f=20MHz, r=70m, $\varphi_0 = 120^{\circ}$).

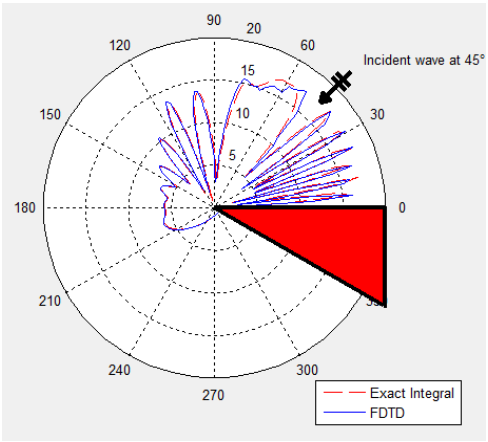

Fig. 12. Total Fields vs. angle solution computed with FDTD, UTD, and Exact integral models ($\alpha = 330^{\circ}$, f=30MHz, r=80m, $\varphi_0 = 45^{\circ}$).

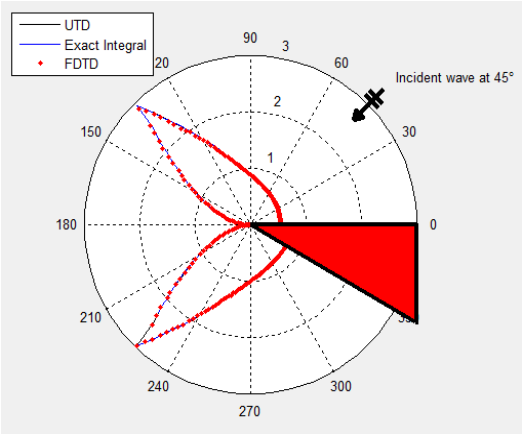

Fig. 13. Diffracted fields vs. angle solution computed with, FDTD, UTD, and Exact integral models ($\alpha = 330^{\circ}$, f=30MHz, r=80m, $\varphi_0 = 45^{\circ}$).

VI. CONCLUSION

A novel Matlab based tool is developed to investigate wedge scattering with the Finite-Difference Time-Domain (FDTD) method. Diffracted fields are extracted and are compared with the results of High Frequency Asymptotic (HFA) models. Dey-Mittra conformal FDTD method is used to eliminate staircase modeling deficiencies and results are presented. Excellent agreement among the models for both cases shows the success of the VV&C procedure [17].

REFERENCES

[1] A. Sommerfeld, "Mathematische Theorie der Diffraction," *Mathematische Annalen,* vol. 16**,** pp. 317-374, 1896.

[2] H. M. Macdonald, *Electric Waves,* The University Press, Cambridge, England, pp. 186-198, 1902

[3] G. D. Malyuzhinets, "Development of Ideas about Diffraction Phenomena," *Soviet Physics-Uspekhi*, vol. 69**,** 2, pp. 5, 1959.

[4] J. B. Keller, "The Geometric Optics Theory of Diffraction," presented at the 1953 McGill Symp. Microwave Optics, *A. F. Cambridge Res. Cen. Rep. TR-59-118* (II), pp. 207-210, 1959.

[5] V. A. Fock, *Electromagnetic Diffraction and Propagation Problems,* Pergamon Press, London, 1965.

[6] R. G. Kouyoumjian and P. H. Pathak, "A Uniform Geometrical Theory of Diffraction for an Edge in a Perfectly Conducting Surface," *Proc. IEEE*, vol. 62, pp. 1448-1461, Nov. 1974.

[7] P. Ya. Ufimtsev, *Theory of Edge Diffraction in Electromagnetics: Origination & Validation of PTD*, SciTech Publishing, Inc., 2009.

[8] P. Ya. Ufimtsev, *Fundamentals of the Physical Theory of Diffraction,* Wiley & Sons, Inc., Hoboken, New Jersey, 2007.

[9] F. Hacıvelioğlu, L. Sevgi, P. Ya. Ufimtsev, "Electromagnetic Wave Scattering from a Wedge with Perfectly Reflecting Boundaries: Analysis of Asymptotic Techniques," *IEEE Antennas and Propagation Magazine*, vol. 53, no. 3, pp. 232-253, Jun 2011.

[10] F. Hacıvelioğlu, M. A. Uslu, L. Sevgi, "A Matlab-based Simulator for the Electromagnetic Wave Scattering from a Wedge with Perfectly Reflecting Boundaries," *IEEE Antennas and Propagation Magazine*, vol. 53, no. 4, pp. 234-243, Dec. 2011.

[11] F. Hacivelioglu, L. Sevgi, "On the Numerical Evaluations of Diffraction Formulas for the Canonical Wedge Scattering Problems," *Applied Computational Electromagnetics Society (ACES) Journal*, 2012. (submitted)

[12] G. Çakır, L. Sevgi, P. Ya. Ufimtsev, "FDTD Modeling of Electromagnetic Wave Scattering from a Wedge with Perfectly Reflecting Boundaries: Comparisons against Analytical Models and Calibration," *IEEE Trans. on Antennas and Propagat.*, 2012. (to appear)

[13] K. S. Yee, "Numerical Solution of Initial Boundary Value Problems Involving Maxwell's Equations in Isotropic Media", *IEEE Trans. Antennas and Propagat*., **14**, pp. 302-307, 1966.

[14] S. Dey, R. Mittra, "A Locally Conformal FDTD Algorithm for Modeling Three-Dimensional Perfectly Conducting Objects," *IEEE Microwave and Guided Wave Letters*, 7 (9), pp. 273-275, Sep. 1997.

[15] C. J. Railton, J. B. Scheider, "An Analytical and Numerical Analysis of Several Locally Conformal FDTD Schemes," *IEEE Trans on MTT*, 47 (1), pp. 56-66, Jan. 1999.

[16] J.J. Bowman, T.B.A. Senior, P.L.E. Uslenghi, *Eds., Electromagnetic and Acoustic Scattering by Simple Shapes*, Hemisphere Publishing Corporation, 1987.

[17] G. Apaydin, L. Sevgi, "Validation, Verification and Calibration in Applied Computational Electromagnetics," *Applied Computational Electromagnetics Society (ACES) Journal*, vol. 25, no. 12, pp. 1026-1035, December 2010.

Mehmet Alper USLU was born in Turkey, in 1986. He received B.S. and M.S. in Electronics and Communication Engineering from Dogus University, Turkey in 2010 and 2012, respectively. Currently, he is pursuing his PhD studies in Institute of Science and Technology of the same university. He is one of the two recipients of Doğuş University-Felsen Fund Excellence in Electromagnetics 2011 award His research interests are diffraction theory, computational electrodynamics, RF Microwave circuits and systems, EMC and Digital signal processing algorithms.

Levent Sevgi (M'99-SM'02-F'09) has been with Dogus University since 2002. He has involved in complex electromagnetic problems for more than two decades. His research study has focused on radar systems, surface wave HF radars, propagation in complex environments, analytical and numerical methods in electromagnetic, EMC/EMI modeling and measurement, FDTD, FEM, TLM, SSPE and MoM techniques and their applications, RCS modeling, bio-electromagnetics. He is also interested in novel approaches in engineering education, teaching electromagnetics via virtual tools, and Science, Technology and Society issues.

He is a member of Turkish Chamber of Electrical Engineers (EMO), an assoc. Editor, of the IEEE Antennas and Propagation Magazine, "Testing ourselves" Column and member of the IEEE Antennas and Propagation Society Education Committee